A Reconfigurable Sound Wave Decomposition Filterbank for Hearing Aids Based on Nonlinear Transformation

Shaoguang Huang, Lan Tian, Xiaojie Ma, and Ying Wei, *Member, IEEE*

***Abstract*—Hearing impaired people have their own hearing loss characteristics and listening preferences. Therefore hearing aid system should become more natural, humanized and personalized, which requires the filterbank in hearing aids provides flexible sound wave decomposition schemes, so that patients are likely to use the most suitable scheme for their own hearing compensation strategy. In this paper, a reconfigurable sound wave decomposition filterbank is proposed. The prototype filter is first cosine modulated to generate uniform subbands. Then by non-linear transformation the uniform subbands are mapped to nonuniform subbands. By changing the control parameters, the nonlinear transformation changes which leads to different subbands allocations. It provides four different sound wave decomposition schemes without changing the structure of the filterbank. The performance of the proposed reconfigurable filterbank was compared with that of fixed filerbanks, fully customizable filterbanks and other existing reconfigurable filterbanks. It is shown that the proposed filterbank provides satisfactory matching performance as well as low complexity and delay, which make it suitable for real hearing aid applications.**

***Index Terms*—Filterbank, hearing aids, reconfigurable.**

I. Introduction

THE main target of hearing aids is to provide proper hearing compensation for people with hearing loss. There are two aspects especially important in this process. The first one is to decompose the inputting sound waves, which is achieved by a filterbank. The second one is to selectively amplify the subband signals. The filterbanks used currently could be divided into two categories, uniform filterbanks and non-uniform filterbanks. Much work has been done in the design of uniform filterbanks for hearing aids [1]–[5]. Due to the non-uniform scaling of human auditory filtering, uniform filterbanks cannot provide satisfactory sound compensation for hearing loss patients. Therefore, much effort was devoted to the non-uniform filterbank design. In [6], a 3-subband non-uniform filterbank was proposed combining with frequency response masking (FRM) technique. The filterbank achieved lower complexity compared with uniform filterbanks. In [7]–[9], with the FRM technique, non-uniform filterbanks were realized. Half-band filters were used as prototype filters, which further reduced the complexity. In [10] and [11], a 3-subband variable filterbank was proposed. A prototype Chebyshev type-I low-pass filter was firstly designed, and then the prototype filter was converted to the low-pass filter, band-stop filter and high-pass filter respectively, using the analog frequency transformations along with a modified bilinear transformation. The maximum matching errors of the audiograms were extremely small. It should be noted that "variable" here means the cut-off frequencies of the parallelizing low-pass, band-pass and high-pass digital filters are variable. The coefficients of the filterbank will be modified as the three converted filters changes. A 16-channel critical band-like spaced filter bank was proposed in [12]. With the common pre-computational unit, a set of intermediate values could be shared by all the channels to achieve low power and small area. In [13], the FIR-based design of the 1/3 octave filter bank was proposed. The multi-rate architecture saved both the power and chip size of hearing aids. A 10-ms 18-band Quasi-ANSI S1.11 1/3 octave filter bank was proposed in [14]. The inter-band interference was reduced by a prescription-fitting algorithm.

Filterbanks mentioned above only provides one kind of sound decomposition scheme. However, the features of hearing loss denoted by audiograms are different from person to person. It is meaningful to provide various sound decompositions to meet the demands of different patients, which implies that the filterbank needs to be reconfigurable. Here "reconfigurable" means that different subbands distributions could be obtained according to the control parameters without changing the filterbank's structure. In [15], a low power digital signal processor for a digital hearing aid chip was proposed, in which a 3-band filterbank was constituted with three programmable digital FIR filters. Each FIR filter had seven available pass-frequencies, so the filterbank had the same flexibility as seven filters. Combining with voice activity detection, the proposed filterbank achieved low power consumption. An adjustable filterbank, which could provide 27 different subbands, was proposed in [16], [17]. The use of FRM technique together with interpolation and decimation made the complexity of filterbank much

Manuscript received January 03, 2015; revised April 07, 2015; accepted May 12, 2015. Date of publication July 08, 2015; date of current version February 29, 2016. This work was supported by the Shandong Province Science and Technology Development Plan (2013GGX10103), the Fundamental Research Funds of Shandong University (2015JC029), the National Natural Science Foundation of China (61201372, 11474185), the Scientific Research Foundation for the Returned Overseas Chinese Scholars, the State Education Ministry, and the Taishan Scholar Foundation Project (1170082963013). This paper was recommended by Associate Editor J. Georgiou.

S. Huang, L. Tian, and Y. Wei are with the School of Information Science and Engineering, Shandong University, Jinan 250100, China (e-mail: eleweiy@sdu.edu.cn).

X. Ma is with the Qilu Hospital of Shandong University, Jinan 250000, China.

Digital Object Identifier 10.1109/TBCAS.2015.2436916

lower. The ability to distribute subbands flexibly made the reconfigurable filter banks achieved better compensation than fixed filterbank. However, the throughout delay of these reconfigurable filterbanks was too large to meet the requirement of the hearing aids. In [18], a16-band reconfigurable non-uniform filterbank was realized by using variable bandwidth filters. Each subband was implemented as a combination of two arbitrary sample rate converters and a fixed bandwidth FIR filter. The reconfigurable filterbank had a better matching error compared with fixed non-uniform filterbank. Two kinds of reconfigurable filterbanks designed for multi-standard wireless communication receiver were proposed in [19] and [20]. The design methods which had a lower complexity could also be used in hearing aid systems when their delays were not too large. In this paper, a low delay reconfigurable filterbank was proposed. Firstly, a uniform filterbank was designed with the cosine modulation technique. Then, the uniform filterbank was converted into non-uniform filterbank by the nonlinear transformation. This can be done through substituting each delay unit of the FIR filter with the cascade of all-pass IIR filters. Finally, by adjusting the control parameter, the reconfigurability of the proposed filterbank was achieved.

The rest of this paper is organized as follows. In Section II, the fundamentals of the idea are described. In Section III, the structure, implementation and gains optimization algorithm of the proposed reconfigurable filterbank are discussed. Design process is shown in Section IV. In Section V, examples are presented to test the effectiveness of the proposed filterbank. Finally, conclusions are drawn in Section VI.

II. Fundamentals of the Idea

Before the structure of the proposed filterbank is presented, the design of cosine modulated filterbank and the nonlinear transformation will be described.

A. Cosine-Modulated Uniform Filterbank

A cosine-modulated filterbank $h^{(i)}(n)$ $(i = 0, \ldots, M)$ is defined as (1), where $h_L(n)$ is a low-pass FIR prototype filter with length L, M is the modulation factor and i is the index of the subband. c_i is a magnitude control factor with $c_i = 1$ for $i = 0, M$ and $c_i = 2$ for $i = 1, \ldots, M-1$. The z-transform transfer function of $h^{(i)}(n)$ is expressed in (2), where $i = 0, 1, \ldots, M$.

$$h^{(i)}(n) = c_i \cdot h_L(n) \cdot \cos\left(\frac{i \cdot \pi}{M} n\right) \tag{1}$$

$$\begin{aligned} H^{(i)}(z) &= \sum_{n=0}^{L-1} h^{(i)}(n) z^{-n} \\ &= \sum_{n=0}^{L-1} c_i \cdot h_L(n) \cdot \cos\left(\frac{i \cdot \pi}{M} n\right) \cdot z^{-n} \end{aligned} \tag{2}$$

The magnitude response of the cosine-modulated filterbank is shown in Fig. 1, where ω_p and ω_s are the passband edge and stopband edge of the low-pass prototype filter, respectively. It is suggested in the figure that to make the sum of the magnitude responses of all the subbands equal to unity, (3) should be satisfied. The structure of the cosine-modulated filterbank expressed by (2) is shown in Fig. 2, where $y^{(i)}(n)$ is the output signal of $x(n)$ passing through $h^{(i)}(n)$. Coefficients of $h_L(n)$ are shared in this structure. The details about the module of cosine modulation will be discussed in the following section.

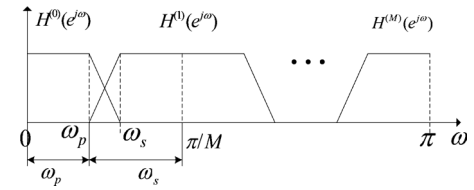

Fig. 1. The cosine-modulated filterbank.

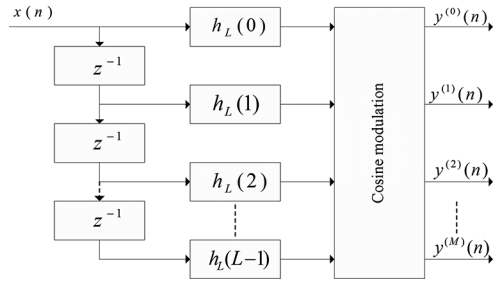

Fig. 2. The structure of the cosine-modulated filterbank.

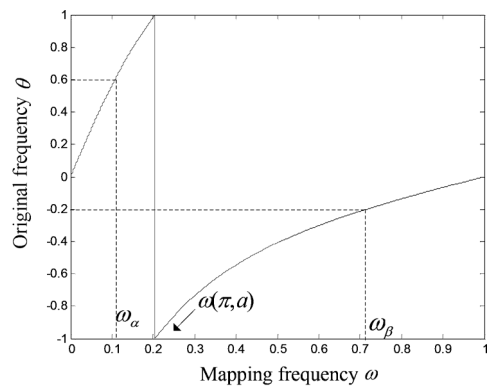

Fig. 3. Nonlinear transformation with $a = 0.5$.

$$\omega_p + \omega_s = \frac{\pi}{M} \tag{3}$$

B. The Nonlinear Transformation

In order to transform the uniform filterbank to a non-uniform filterbank, the original coordinate axis is mapped to a new coordinate axis by a nonlinear transformation, shown in (4).

$$\begin{aligned} z^{-1} = G(Z^{-1}) &= \frac{Z^{-1} - a}{1 - a^* \cdot Z^{-1}} \cdot \frac{Z^{-1} - a^*}{1 - a \cdot Z^{-1}} \\ &= \frac{Z^{-2} + d_1 \cdot Z^{-1} + d_2}{d_2 \cdot Z^{-2} + d_1 \cdot Z^{-1} + 1} \end{aligned} \tag{4}$$

where z and Z are the z-transform symbols in the original space and the transformed space, respectively. $G(Z^{-1})$ is the cascade of two all-pass filters. Assuming that θ is the frequency point in the original space and ω is the mapped frequency point of θ

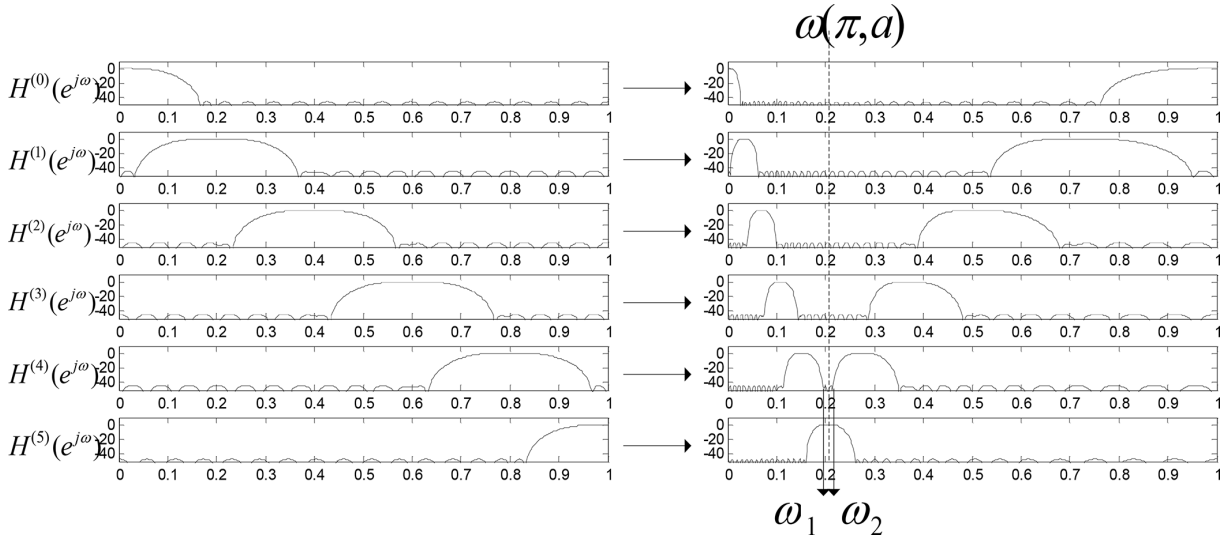

Fig. 4. Passband generation from uniform filterbank.

in the transformed space, where $-\pi < \theta \leq \pi$, $-\pi < \omega \leq \pi$. Substituting $z = e^{j\theta}$ and $Z = e^{j\omega}$ into (4), we have

$$e^{-j\theta} = \frac{e^{-j2\omega} + d_1 \cdot e^{-j\omega} + d_2}{d_2 \cdot e^{-j2\omega} + d_1 \cdot e^{-j\omega} + 1}. \tag{5}$$

Solving (5), we have

$$\sin\omega = \frac{-q \pm \sqrt{q^2 - 4ps}}{2p} \tag{6}$$

where

$$p = 8d_2 \cos\theta - 4 - 4d_2^2 \tag{7}$$
$$q = 4d_1(1 - d_2) \cdot \sin\theta \tag{8}$$
$$s = 2(1 + d_1 + d_2)(1 - d_1 + d_2)(1 - \cos\theta). \tag{9}$$

Let us denote a in (4) as

$$a = r \cdot \cos\varphi + j \cdot r \cdot \sin\varphi, (0 \leq r < 1, 0 \leq \varphi \leq \pi) \tag{10}$$

we have

$$d_1 = -(a + a^*) = -2 \cdot r \cdot \cos\varphi \tag{11}$$
$$d_2 = a \cdot a^* = r^2. \tag{12}$$

Among the four solutions for (6), only two of them satisfy (5). For the solutions that satisfy (5), we care about the positive one. Since d_1, d_2 can be expressed by a, we denote the positive mapping frequency point as $\omega(\theta, a)$.

Let us illustrate the non-linear transformation by an example. The transformation described by (5) with $a = 0.5$ is shown in Fig. 3, in which the frequencies are normalized by π. We can see that $\theta \in (-\pi, \pi)$ is mapped to $\omega \in (0, \pi)$. The frequencies in the original space are compressed in the areas where the gradient of mapping line is larger than 1 and are expanded in the areas where gradient of mapping line is less than 1. For example, $\theta \in [0, 0.6\pi]$ is compressed into $\omega \in [0, \omega_\alpha]$ where $\omega_\alpha < 0.6\pi$ and the range $\theta \in [-0.2\pi, 0]$ is expanded into $\omega \in [\omega_\beta, \pi]$ where $\omega_\beta < 0.8\pi$. In general $\theta \in (-\pi, 0)$ is mapped into $\omega \in (\omega(\pi, a), \pi)$ and $\theta \in (0, \pi)$ is mapped to $\omega \in (0, \omega(\pi, a))$. In this example $\omega(\pi, a)$ equals to 0.2048π.

Substituting (4) into $H^{(i)}(z)$ yields a new band allocation as shown in Fig. 4. It should be noted that one original passband is mapped into two passbands. In order to separate the mapped subband pairs to get the individual subband, a low-pass filter $h_m(n)$ and its complementary filter are used as the masking filters. Its passband edge ω_1 and stopband edge ω_2 can be easily obtained by

$$\omega_1 = \omega(\omega_{t_1}, a) \tag{13}$$
$$\omega_2 = \omega(-\omega_{t_1}, a) \tag{14}$$

where ω_{t_1} is the right stopband edge of the subfilter $H^{(M-1)}(z)$

$$\omega_{t_1} = \frac{M-1}{M}\pi + \omega_s. \tag{15}$$

III. Proposed Reconfigurable Non-Uniform Filterbank

A. The Influence of Parameter a on the Band Allocations

The purpose of this work is to provide hearing aid systems a reconfigurable sound wave decomposition in accordance with the hearing loss characteristic of patients. "Reconfigurability" here means the filterbank provides various band allocation schemes without changing the coefficients and the structure. The block diagram of this idea is shown in Fig. 5. It consists of two parts, passbands generation and masking. By changing the value of parameter a, the non-linear transformation introduced by (4) changes, which results in different band allocation schemes as defined in Table I. Here the value of a is adjusted in accordance with parameter W. In addition, for different a, different masking filters are needed.

For a certain $a = r \cdot \cos\varphi + j \cdot r \cdot \sin\varphi$, the generated scheme is related to both r and φ. There are three important observations about parameter a,

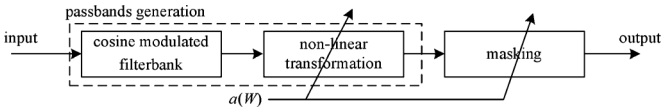

Fig. 5. The diagram of the idea of "Reconfigurability".

TABLE I
DIFFERENT BAND ALLOCATION SHEMES

Scheme	Band allocation
1	nonuniform subbands with narrower subbands in low frequencies
2	nonuniform subbands with narrower subbands in high frequencies
3	nonuniform subbands with narrower subbands in middle frequencies
4	uniform subbands

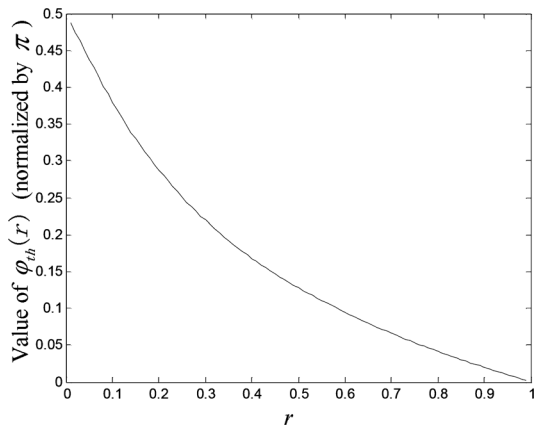

Fig. 6. The value of $\varphi_{\rm th}(r)$ for different r.

1) $\omega(\theta, a) + \omega(-\theta, -a) = \pi$, that means, the frequency response of the non-uniform filterbank with the parameter a is the mirror image at $\pi/2$ with that of the non-uniform filterbank with parameter $-a$.
2) When a is not equal to zero, schemes 1, 2 and 3 are all possible. In accordance with (6), there is a threshold $\varphi_{\rm th}(r)$ to determine the schemes. If $\varphi \in [0, \varphi_{\rm th}(r))$, scheme 1 is produced. If $\varphi \in (\pi - \varphi_{\rm th}(r), \pi]$, scheme 2 is produced. If $\varphi \in [\varphi_{\rm th}(r), \pi - \varphi_{\rm th}(r)]$, scheme 3 is produced. The value of $\varphi_{\rm th}(r)$ for different r is plotted in Fig. 6.
3) Especially, when a is a pure imaginary number or equal to zero, frequency response of the proposed filterbank is symmetric at $\pi/2$. If $a = j \cdot r (\varphi = \pi/2)$, scheme 3 is generated. If $a = 0$, scheme 4 is generated.

B. The Structure of the Proposed Filterbank

In order to use the property of symmetry to reduce the complexity of the masking filters, the proposed filterbank is designed to provide four band allocation schemes shown in Table I in accordance with the values of a in Table II.

Observation (1) together with the (13) and (14) suggests that the masking filter for scheme 1 is symmetric at $\pi/2$ with the masking filter for scheme 2. Therefore the masking filter for scheme 2 can be produced by changing the sign of the coefficients of the masking filter for scheme 1 alternatively. They can share the multipliers used. Observation (3) suggests that when a is a pure imaginary number or equal to zero, the allocation of subbands is symmetric to $\pi/2$. Therefore half-band filters can be employed for masking, which will reduce the complexity of the filterbank greatly. In fact, for scheme 3 and 4, they can share the masking filter with a narrower transition bandwidth among the two half-band filters. Based on above analysis, it is possible to use only two prototype masking filters for all the schemes.

TABLE II
VALUES OF a FOR DIFFERENT SCHEMES

Scheme	Value of a	Values of r and φ
1	$r \cdot \cos\varphi + j \cdot r \cdot \sin\varphi$	$0 < r < 1, \varphi \in [0, \varphi_{th}(r))$
2	$-r \cdot \cos\varphi - j \cdot r \cdot \sin\varphi$	$0 < r < 1, \varphi \in [0, \varphi_{th}(r))$
3	$j \cdot r$	$0 < r < 1, \varphi = \pi / 2$
4	0	$r = 0$

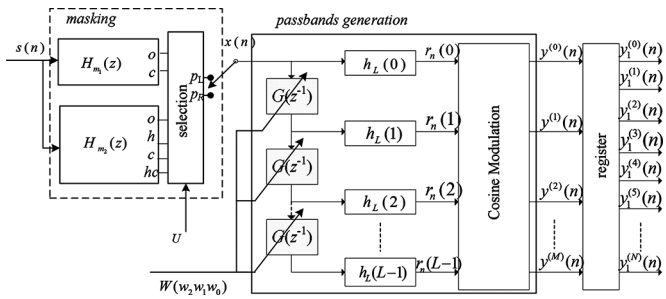

Fig. 7. The proposed reconfigurable non-uniform filterbank.

The structure of the proposed reconfigurable filterbank is shown in Fig. 7. Since changing the cascading order does not change the output of the filterbank, the masking part is put in front of the passbands generation part.

The nonlinear transformation is done by replacing the delay element z^{-1} in the cosine modulated filterbank in Fig. 2 with $G(z^{-1})$. $H_{m_1}(z)$ is the half-band prototype masking filter for scheme 3 and 4. The block based on $H_{m_1}(z)$ has two output ports. The mark "o" denotes the original output of the half-band filter $H_{m_1}(z)$ and the mark "c" denotes its complement output. $H_{m_2}(z)$ is the prototype masking filter for scheme 1 and 2. To extract the subbands of scheme 1, $H_{m_2}(z)$ and its complement filter are used. Since the subbands of scheme 2 are symmetric at $\pi/2$ with the subbands of scheme 1, the masking filters for scheme 2 are symmetric at $\pi/2$ with the masking filters for scheme 1. Therefore, there are four ports in the masking block based on $H_{m_2}(z)$. The meaning of the ports "o", "c", "h" and "hc" in Fig. 7 is listed in Table III. Considering the relationships among the outputs, the target filters could be obtained by sharing the same set of multipliers and part of the delays. The details of implementation will be discussed in Section C.

The output of the masking stage is determined by a 1-bit control parameter U. When $U = 0$, p_L is chosen and half number of subbands in low frequencies are extracted. When $U = 1$, p_R is chosen and half number of subbands in high frequencies are extracted. For each W which determines the scheme, U equals to 0 and 1 in turn. Therefore, all the subbands can be obtained. The outputs of ports p_L and p_R for different schemes are shown in Table IV. It should be noted that the last mapped subband, as

TABLE III
THE MEANING OF DIFFERENT PORTS

Port	Meaning	Magnitude response of the target filter
o	output of the original filter	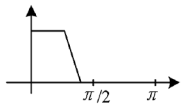
c	output of the complement filter	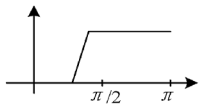
h	output of the filter symmetric with the original filter at $\pi/2$	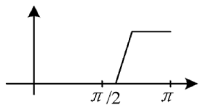
hc	output of the complement filter of the filter symmetric with the original filter at $\pi/2$	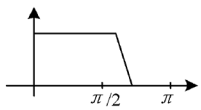

TABLE IV
THE OUTPUT PORTS FOR DIFFERENT SCHEMES

scheme	port p_L (U=0)	port p_R (U=1)
1	output of port "*o*" of $H_{m_2}(z)$ block	output of port "c" of $H_{m_2}(z)$ block
2	output of port "*hc*" of $H_{m_2}(z)$ block	output of port "*h*" of $H_{m_2}(z)$ block
3 and 4	output of port "*o*" of $H_{m_1}(z)$ block	output of port "*c*" of $H_{m_1}(z)$ block

shown in the bottom of Fig. 4, is also separated into two portions. By simple addition of them, a full subband can be easily obtained. Overall, the total number of subbands, N, is equal to $2M+1$.

C. Implementation

In this part, let us discuss the implementation of the masking block, the nonlinear transformation $G(z^{-1})$ and the cosine modulation. For the masking block, there are original filter, complement filter, symmetric filter at $\pi/2$ and complement filter of the symmetric filter. All these filters can be implemented by sharing

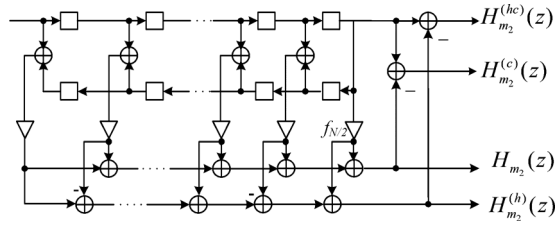

Fig. 8. The implementation of the making block.

the multipliers as shown in Fig. 8. Therefore, the complexity can be reduced greatly.

For the implementation of the cosine modulation, let us look at the output of the filterbank first. The output is expressed by (16), where $x(n)$ is the output of the masking block.

$$\begin{aligned} y^{(i)}(n) &= \sum_{k=0}^{L-1} x(n-k)\cdot h^{(i)}(k) \\ &= \sum_{k=0}^{L-1} x(n-k)\cdot c_i \cdot h_L(k)\cdot \cos\left(\frac{i\cdot\pi}{M}k\right) \\ &= c_i \cdot \sum_{k=0}^{M-1} x_n^{(i)}(k)\cdot \cos\left(\frac{i\cdot\pi}{M}k\right) \\ &= c_i \cdot \sum_{k=0}^{M-1} x_n^{(i)}(k)\cdot \cos\left(\theta_k^{(i)}\right) \end{aligned} \tag{16}$$

Due to the periodicity of cosine function, $x_n^{(i)}(k)$ is expressed as follows, where [see (17)–(19) at the bottom of the page.]

Based on these equations, the structure of cosine modulation with $L = sM$ can be illustrated in Fig. 9. It's similar for $L \neq sM$. Moreover, the multiplier in the end of cosine modulation can be replaced with adder for the value of c_i is 1 or 2. Therefore, the number of multipliers in the cosine modulation is equal to $M\cdot(M+1)$.

Then, let us discuss the realization of the reconfigurability of the filterbank. If the parameter a is selected elaborately, as shown in Table II, the reconfigurable structure is possible.

For scheme 1, since $a = r\cdot\cos\varphi + j\cdot r\cdot\sin\varphi$, based on (11) and (12), we have

$$\begin{aligned} d_1 &= -2\cdot r\cdot\cos\varphi, \\ d_2 &= r^2. \end{aligned}$$

$$x_n^{(i)}(k) = \begin{cases} r_n(k)+\cdots+(-1)^{i(s-1)}\cdot r_n(k+(s-1)M), & L = sM \\ r_n(k)+\cdots+(-1)^{is}\cdot r_n(k+sM), & L = sM+t \,\&\, 0 \le k \le t-1 \\ r_n(k)+\cdots+(-1)^{i(s-1)}\cdot r_n(k+(s-1)M), & L = sM+t \,\&\, k \ge t \end{cases} \tag{17}$$

$$\theta_k^{(i)} = \frac{i\cdot\pi}{M}k \tag{18}$$

$$r_n(k) = x(n-k)\cdot h_L(k). \tag{19}$$

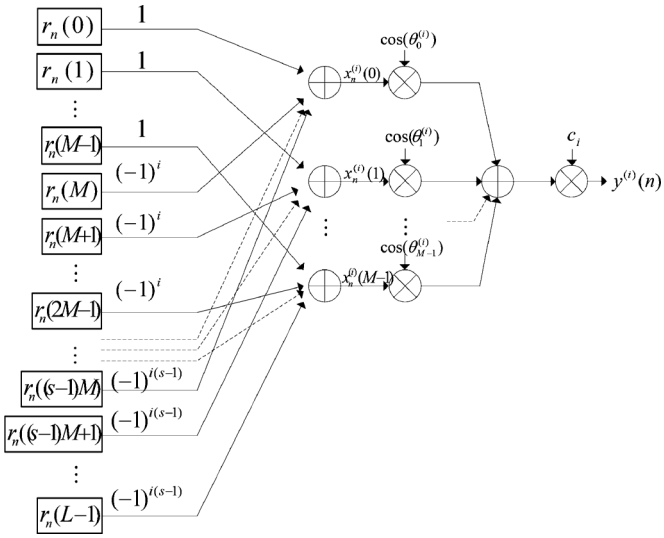

Fig. 9. The cosine modulation for $L = sM$.

For scheme 2, since $a = -r \cdot \cos\varphi - j \cdot r \cdot \sin\varphi$, we have

$$d_1 = -(a + a^*) = 2 \cdot r \cdot \cos\varphi \tag{20}$$

$$d_2 = a \cdot a^* = r^2. \tag{21}$$

For scheme 3, since $a = j \cdot r$, we have

$$d_1 = -(a + a^*) = 0 \tag{22}$$

$$d_2 = a \cdot a^* = r^2. \tag{23}$$

For scheme 4, since $a = 0$, we have

$$d_1 = -(a + a^*) = 0 \tag{24}$$

$$d_2 = a \cdot a^* = 0. \tag{25}$$

In accordance with above analysis, the reconfiguability can be achieved by the structure shown in Fig. 10. The change of value of a is achieved by controlling the switches, which contributes to the reconfigurability of the filter bank. $G(z^{-1})$ for the four schemes can be realized by adjusting the status of the switches S_1, S_2 and S_3. The statuses of the switches for the four schemes are shown in Table V.

Based on the above structure, the total number of multipliers in the proposed filterbank is expressed by

$$\begin{aligned} N_{\text{total}} &= N_{hl} + N_{\text{cosine}} + N_{\text{nonlinear}} + N_{hm1} + N_{hm2} \\ &= L + M \cdot (M+1) + 3 \cdot (L-1) \\ &\quad + (L_{m_1} + 1)/4 + \lceil L_{m_2}/2 \rceil \\ &= 4 \cdot L + (L_{m_1} + 1)/4 + \lceil L_{m_2}/2 \rceil \\ &\quad + M \cdot (M+1) - 3 \end{aligned} \tag{26}$$

where L_{m_1} and L_{m_2} denote the length of $H_{m_1}(z)$ and $H_{m_2}(z)$, respectively. The estimation of the length of FIR filter is performed by the method in [21].

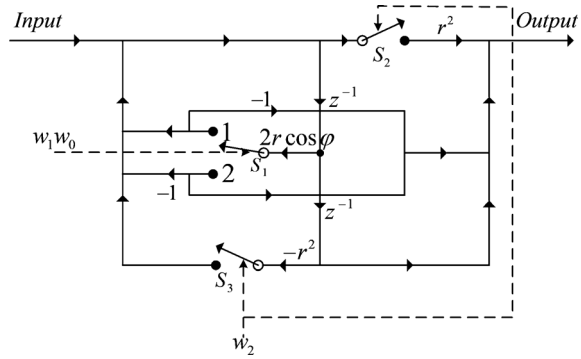

Fig. 10. The reconfigurable module of $G(z^{-1})$.

TABLE V
STATUS OF THE SWITCHES FOR DIFFERENT SCHEMES

Scheme	$W(w_2w_1w_0)$	S_3	S_2	S_1
1	101	closed	closed	connects to 1
2	110	closed	closed	connects to 2
3	100	closed	closed	open
4	000	open	open	open

D. Optimization for the Gains in Each Subband

After getting the $2M + 1$ subbands with the above filterbank, optimization for the gain of each subband will be performed to minimize the maximum matching error between the frequency response of the whole system and a given audiogram. The zero-phase frequency response of overall system can be written as

$$H_{\text{total}}(\omega) = \sum_{i=0}^{N-1} \widehat{G_i} \cdot H_u^{(i)}(\omega) \tag{27}$$

where $H_u^{(i)}(\omega)$ denotes the zero-phase frequency response of the ith subband, $\widehat{G_i}$ is the gain of the ith subband.

For example, an audiogram for fine hearing is shown in Fig. 11. The two marked curves denote the hearing thresholds $M_d(\widehat{f_i})$ of left ear and right ear, respectively, which are usually measured in decibels (dB) at the frequencies $\widehat{f_i} = 250/500/1\text{k}/2\text{k}/4\text{k}/8$ k. The denser points $M_d(f_i)$ can be obtained by linear interpolation in dB, where

$$M_d(f_i) = M_d(\widehat{f_i}), \quad \text{if } f_i = \widehat{f_i}. \tag{28}$$

Transform the analog frequency f_i to digital frequency ω_i by $\omega_i = (2\pi f_i)/(f_s)$, where f_s is the sample frequency. To obtain the gains G_i for each subband, following cost function should be minimized.

$$E = \max_{\omega_i \in [0,\pi]} |H_{\text{total}}(\widehat{G_i}, \omega_i) - M_d(\omega_i)| \tag{29}$$

The problem in (29) is known as a *minimax* problem which can be solved with the function *fminimax* from the optimization toolbox provided by MathWorks, Inc [22]. It is important to note that the recruitment-phenomenon [23] is not considered here. In a real application, the recruitment- phenomenon must be taken into consideration. The gain formulas such as NAL-NL2, DSLv5, and CAM2 should be used.

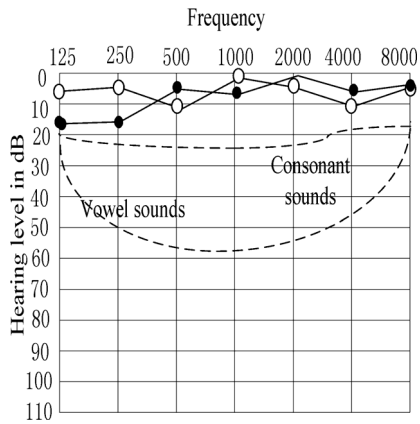

Fig. 11. Audiogram for fine hearing.

TABLE VI
THE PARAMETERS OF THE PROPOSED FILTERBANK

Module	Parameter
Nonlinear transformation $G(z^{-1})$	a (r and φ)
Prototype filter $H_L(z)$ for the cosine modulated filterbank	Band edges ω_p, ω_s and M
Prototype filter $H_{m_1}(z)$ for masking	Band edges ω_{pm1} and ω_{sm1}
Prototype filter $H_{m_2}(z)$ for masking	Band edges ω_{pm2} and ω_{sm2}

IV. DESIGN PROCESS

There are several parameters needed to be calculated in the design process. These parameters are listed in Table VI.

The proposed reconfigurable filterbank can be designed with the following steps.

1) Determine the value of $M(M > 1)$. If at least N_b subbands are needed, $M = \lceil (N_b - 1)/2 \rceil$.
2) Estimate the total number of multipliers N based on parameters a ($0 < r < 1$ and $0 \le \varphi < \varphi_{\rm th}$) for nonlinear transformation and the band edges (ω_p, ω_s) of $H_L(z)$. This is done by a global search. For a certain set of $[r, \varphi, \omega_p]$, ω_s can be firstly obtained by (3). Then based on $a = r \cdot \cos\varphi + j \cdot r \cdot \sin\varphi$ and $a = j \cdot r$, the band edges of the masking filters $H_{m_2}(z)$ and $H_{m_1}(z)$ can be calculated by (13) and (14), respectively. In accordance with these specifications, the lengths of the subfilters are estimated by [21]. Then the total number of multipliers, N, is obtained by (26). Fig. 12 is an example with $M = 3$ to illustrate the relationship between the total complexity N and parameters r, φ and ω_p.

   There exists optimum values of ω_p and φ resulting in the estimated lowest complexity of the filterbank for a certain r. The larger the value of r is, the larger the total number of multipliers is. The larger the value of r is, the greater the difference of the bandwidths (non-uniformity) of the subbands is. Considering both the complexity and the non-uniformity, it's recommended to take the value of r between 0 and 0.4. Here the interval of r is set to be 0.05. Therefore, eight sets of $[r_i, \omega_{p_i}, \varphi_i]$ are available for the following design.

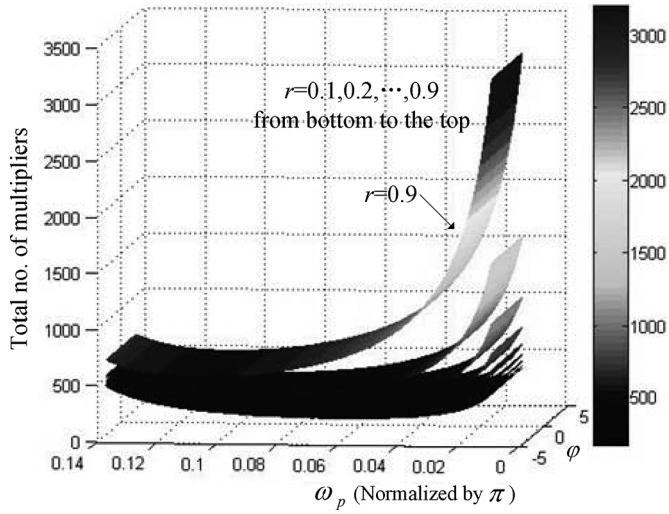

Fig. 12. No. of multipliers with different values of r and ω_p.

3) Find the solution. For each set of $[r_i, \omega_{p_i}, \varphi_i]$, perform the gain optimization algorithm mentioned above and calculate the minimum value of E defined in (29) for different audiograms. Among the various cases of $[r_i, \omega_{p_i}, \varphi_i]$, we choose the one with which the average matching error is smallest.

V. DESIGN EXAMPLE

In this section, three typical audiograms are used to design the proposed filterbank. The audiograms are obtained from the Independent Hearing Aid Information, a public service by Hearing Alliance of America. Three different types of audiograms, mild hearing loss in high frequencies (audiogram 1), mild hearing loss in the whole frequencies (audiogram 2) and moderate hearing loss in low frequencies (audiogram 3), are shown in Figs. 13(a), 14(a) and 15(a), respectively. Here, the right ear hearing thresholds (represented by "O") are chosen to be the target of matching.

Suppose we want to design a 7-band system, M equals to 3. Altogether 28 different subbands can be generated. The maximum ripple and stopband attenuation of the subbands are 0.005 and -50 dB, respectively. The filterbank is realized in accordance with the design process described above. The eight sets of parameters and the corresponding average matching error (AME) are shown in Table VII. We choose the filterbank with $[r, \omega_p, \varphi] = [0.3, 0.062\pi, 0.2\pi]$ which has a better matching result as the solution. The length of subfilters $H_L(z)$, $H_{m_1}(z)$ and $H_{m_2}(z)$ are 25,103 and 103, respectively.

The matching results for the audiograms are shown in Figs. 13 to 15. The performance of the proposed filterbank and other types of filterbanks for hearing aids are listed in Table VIII, where MMME means the minimum maximum matching error. Compared to the fixed non-uniform filterbank in [8], the AME and the delay of the proposed filterbank are reduced by 57.8% and 40.2%, respectively, at the same time the complexity is also reduced by 15.2%. Compared to the reconfigurable filterbank in [17], the AME and the delay of the proposed filterbank are reduced by 28.6% and 73.2%,

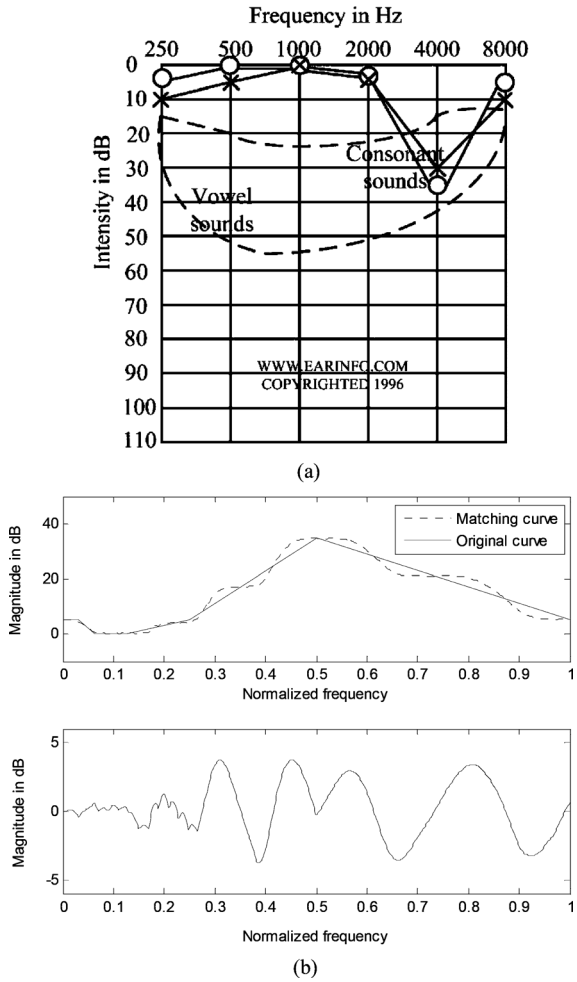

Fig. 13. (a) Audiogram 1: for mild hearing loss in the high frequencies. (b) Matching result and matching error.

respectively. In fact the reconfigurable filterbank in [17] is not suitable for a real hearing aid application due to its large delay. On the contrary, the proposed filterbank can be implemented in practice since the delay is acceptable though it is at a cost of complexity compared to that of the filterbank in [17]. We also listed the experiment results in [10]. The performance of the proposed algorithm does not outperform the algorithm in [10]. In [10], for each audiogram, a three channel filterbank with a new set of coefficients is used, which leads to an extremely low AME and group delay. Such full customization is ideal but too expensive to be widely used in current applications. In conclusion, it is shown by the experiments that the proposed filterbank provides satisfactory matching performance as well as acceptable complexity and delay, which make it suitable for real hearing aid applications.

The advantage of the proposed filterbank lies in two aspects. One is its flexibility that comes from the careful design of a reconfigurable nonlinear transformation. It provides multiple choices of sound wave decomposition schemes, which makes it capable of meeting the different requirements of different kinds of hearing losses. The other one is that compared with other reconfigurable filterbanks, it has smaller delay, which is crucial for practical applications. However, due to the usage of nonlinear transformation, the phase response of the whole system is no longer strictly linear. Fortunately, the requirement of linear phase in audio filtering is not as high as that in areas such as image filtering because human is not sensitive to the phase distortion [10].

TABLE VII
THE RESULTS OF THE PROPOSED METHOD

r	ω_p	N_{total}	φ	AME(dB)
0.05	0.062 π	175	0	2.97
0.10	0.062 π	175	0	2.80
0.15	0.062 π	178	0.1 π	2.61
0.20	0.061 π	181	0.2 π	2.55
0.25	0.062 π	183	0	2.39
0.30	0.062 π	187	0.2 π	2.25
0.35	0.069 π	192	0.2 π	2.30
0.40	0.069 π	198	0.05 π	2.45

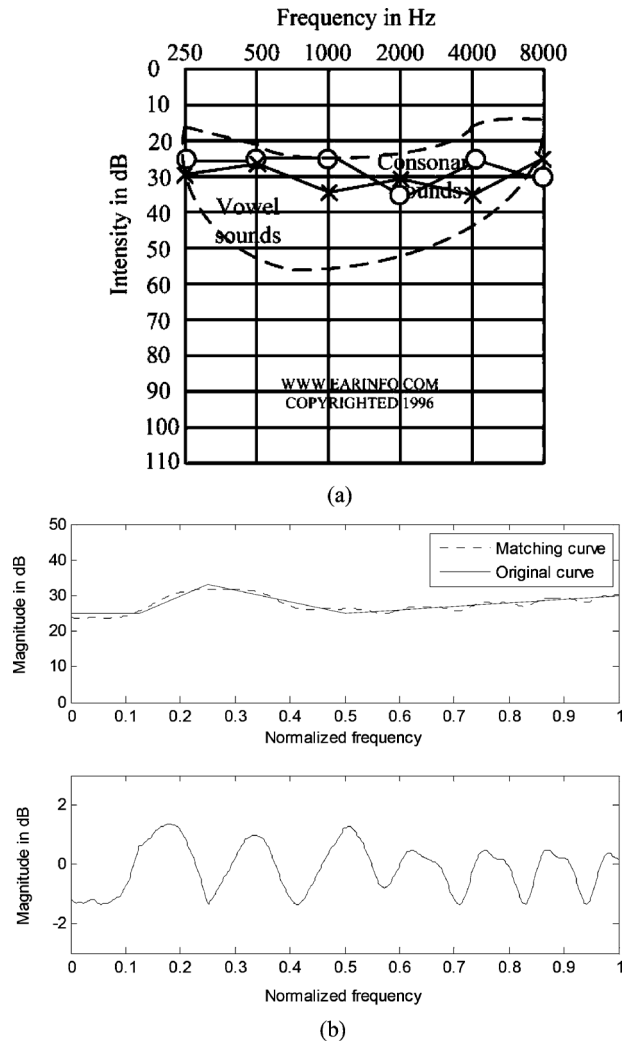

Fig. 14. (a) Audiogram 2: for mild hearing loss in all frequencies. (b) Matching result and matching error.

VI. CONCLUSION

This paper proposed a reconfigurable non-uniform filterbank for hearing aid. The reconfigurable filterbank is based on

TABLE VIII
THE PERFORMANCES FOR VARIOUS FILTERBANKS

filterbank	basic idea	MMME for audiogram 1	MMME for audiogram 2	MMME for audiogram 3	AME	$\frac{No.\ of\ multipliers}{No.\ of\ subbands}$	maximum group delay (16k Hz sample frequency)
ref[8]	non-uniform, fixed subbands, one filterbank for all the audiograms.	9.61 dB	3.7 dB	2.7 dB	5.34 dB	63/8=7.88	13ms
ref [10]	variable subbands, different filterbanks for different audiograms.	2.96 dB	1.68 dB	0.96 dB	1.87 dB	11/3=3.67	2.1ms
ref[17]	reconfigurable subbands, one filterbank for all the audiograms.	4.82 dB	2.67 dB	2.54dB	3.15 dB	90/21=4.29	29ms
proposed	reconfigurable subbands, one filterbank for all the audiograms.	3.75 dB	1.35 dB	1.65 dB	2.25 dB	187/28=6.68	7.77ms

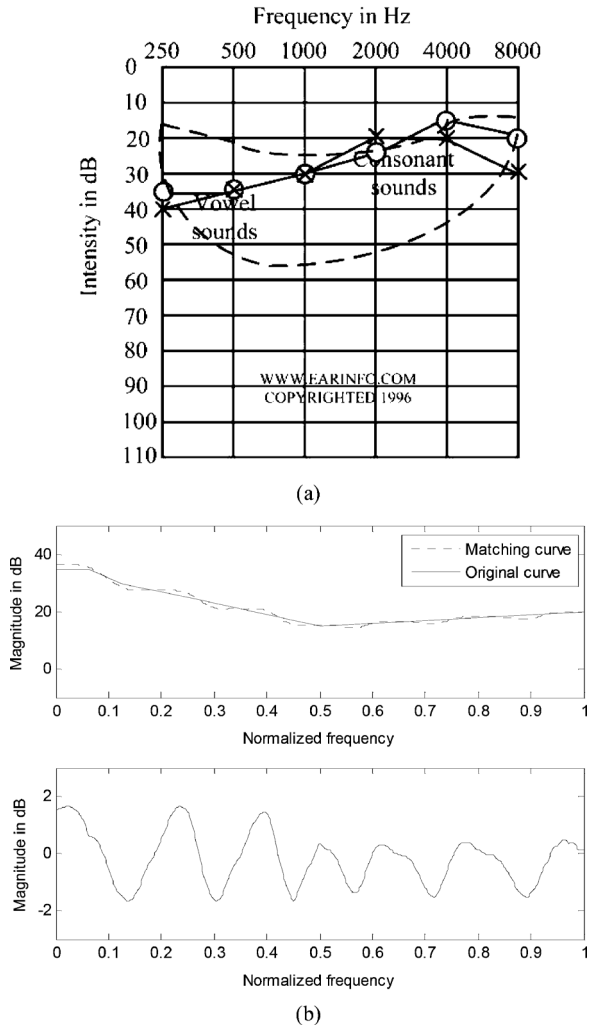

Fig. 15. (a) Audiogram 3: for mild to moderate hearing loss in low frequencies. (b) Matching result and matching error.

cosine-modulated filterbank and non-linear transformation. By adjusting the control parameters, four different types of subband allocations with the same structure are available to supply various sound compensation schemes. Design examples showed that the proposed fitlerbank has better matching results and smaller group delay than recent approaches.

APPENDIX

In this Appendix, we present the derivation of (6) as shown below.

$$e^{-j\theta} = \frac{e^{-j2\omega} + d_1 e^{-j\omega} + d_2}{d_2 e^{-j2\omega} + d_1 e^{-j\omega} + 1} \tag{1}$$

After rearranging the formula (1), we have

$$e^{j2\omega}(1 - d_2 e^{j\theta}) + e^{j\omega} d_1 (1 - e^{j\theta}) + d_2 - e^{j\theta} = 0. \tag{2}$$

By using Euler's formula $e^{j\omega} = \cos(\omega) + j\sin(\omega)$ in (2) and making the real part and imaginary part equal to zero respectively, equations (3) and (4) are derived.

$$(d_2\cos\theta - 1)\cos 2\omega + (d_1\cos\theta - d_1)\cos\omega - d_1\sin\theta\sin\omega - 2d_2\sin\theta\sin\omega\cos\omega + \cos\theta - d_2 = 0 \tag{3}$$

$$2(d_2\cos\theta - 1)\sin\omega\cos\omega + (d_1\cos\theta - d_1)\sin\omega + d_2\sin\theta\cos 2\omega + d_1\sin\theta\cos\omega + \sin\theta = 0 \tag{4}$$

With (3) we obtain

$$\cos\omega = -\frac{\sin\omega\cdot d_1\cdot\sin\theta + 2\sin^2\omega\cdot(d_2\cos\theta - 1)}{d_1(1-\cos\theta) + 2\sin\omega\cdot d_2\cdot\sin\theta} - \frac{(1+d_2)(1-\cos\theta)}{d_1(1-\cos\theta) + 2\sin\omega\cdot d_2\cdot\sin\theta}. \tag{5}$$

By plugging (5) into (4), we get

$$\left(8d_2\cos\theta - 4 - 4d_2^2\right)\sin^2\omega + 4d_1(1-d_2)\sin\theta\sin\omega + 2(1+d_2+d_1)(1+d_2-d_1)\cos\theta = 0. \tag{6}$$

By solving the quadratic equation, the following solution is obtained:

$$\sin\omega = \frac{-q \pm \sqrt{q^2 - 4ps}}{2p} \tag{7}$$

where

$$p = 8d_2\cos\theta - 4 - 4d_2^2 \tag{8}$$

$$q = 4d_1(1-d_2)\cdot\sin\theta \tag{9}$$

$$s = 2(1+d_1+d_2)(1-d_1+d_2)(1-\cos\theta). \tag{10}$$

REFERENCES

[1] Y. C. Lim, "A digital filter bank for digital audio systems," *IEEE Trans. Circuits Syst.*, pp. 848–849, 1986.

[2] L. Thomas and J. Hellgren, "A digital filterbank hearing aid-design, implementation and evaluation," in *Proc. IEEE Int. Conf. Acoustics, Speech, and Signal Processing*, 1991, vol. 5, pp. 3661–3664.
[3] E. Onat, M. Ahmadi, G. A. Jullien, and W. C. Miller, "Optimized delay characteristics for a hearing instrument filter bank," in *Proc. 43rd IEEE Midwest Symp. Circuits and Systems*, Aug. 2000, vol. 3, pp. 1074–1077.
[4] H. Li, G. A. Jullien, V. S. Dimitrov, M. Ahmadi, and W. Miller, "A 2-digit multidimensional logarithmic number system filterbank for a digital hearing aid architecture," in *Proc. IEEE Int. Symp. Circuits and Systems*, 2002, pp. II-760–763.
[5] B. Robert and T. Schneider, "An ultra low-power DSP system with a flexible filterbank," in *Proc. 35th IEEE Asilomar Conf. Signals, Systems and Computers*, 2001, vol. 1, pp. 809–813.
[6] C. Z. Yang and Y. Lian, "A new digital filter bank for digital audio applications," in *Proc. 7th IEEE Int. Symp. Signal Processing and Its Applications*, 2003, vol. 2, pp. 267–270.
[7] Y. Wei and Y. Lian, "A computationally efficient non-uniform digital FIR filter bank for hearing aid," in *Proc. IEEE Int. Workshop Biomedical Circuits and Systems*, 2004, S1.3. INV-17-2.
[8] Y. Lian and Y. Wei, "A computationally efficient nonuniform FIR digital filter bank for hearing aids," *IEEE Trans. Circuits Syst. I, Reg. Papers*, vol. 52, pp. 2754–2762, 2005.
[9] Y. Wei and Y. Lian, "A 16-band nonuniform FIR digital filterbank for hearing aid," in *Proc. IEEE Biomedical Circuits and Systems Conf.*, 2006, pp. 186–189.
[10] T. B. Deng, "Three-channel variable filter-bank for digital hearing aids," *IET Signal Process.*, vol. 4, no. 2, pp. 181–196, Apr. 2010.
[11] N. Ito and T.-L. Deng, "Variable-bandwidth filter-bank for low-power hearing aids," in *Proc. 3rd Int. Congr. Image Signal Processing*, 2010, pp. 3207–3201.
[12] K. S. Chong, B. H. Gwee, and J. S. Chang, "A 16-channel low-power nonuniform spaced filter bank core for digital hearing aid," *IEEE Trans. Circuits Syst.*, vol. 53, no. 9, pp. 853–857, Sep. 2006.
[13] K. Yu-Ting *et al.*, "Complexity-effective auditory compensation for digital hearing aids," in *Proc. IEEE Int. Symp. Circuits and Systems*, 2008, pp. 1472–1475.
[14] C.-W. Liu, K.-C. Chang, M.-H. Chuang, and C.-H. Lin, "10-ms 18-band Quasi-ANSI S1.11 1/3-octave filter bank for digital hearing aids," *IEEE Trans. Circuits Syst. I, Reg. Papers*, vol. 60, no. 3, pp. 638–649, 2013.
[15] S. J. Lee, S. Kim, and H.-J. Yoo, "A low power digital signal processor with adaptive band activation for digital hearing aid chip," in *Proc. IEEE Int. Symp. Circuits and Systems*, 2007, pp. 2730–2733.
[16] Y. Wei and D. Liu, "A design of digital FIR filter banks with adjustable subband distribution for hearing aids," in *Proc. 8th Int. Conf. Information, Communication and Signal Processing*, Singapore, Dec. 13–16, 2011, pp. 361–364.
[17] Y. Wei and D. Liu, "A reconfigurable digital filterbank for hearing-aid systems with a variety of sound wave decomposition plans," *IEEE Trans. Biomed. Eng.*, vol. 60, no. 6, pp. 1628–1635, Jun. 2013.
[18] J. T. George and E. Elias, "A 16-band reconfigurable hearing aid using variable bandwidth filters," *Global J. Researches Eng.*, vol. 14, no. 1, pp. 1–7, 2014.
[19] R. Mahesh and A. P. Vinod, "Reconfigurable low area complexity filter bank architecture based on frequency response masking for nonuniform channelization in software radio receivers," *IEEE Trans. Aerosp. Electron. Syst.*, vol. 47, no. 2, pp. 1241–1255, 2011.
[20] S. J. Darak, J. Palicot, H. Zhang, A. P. Vinod, and C. Moy, "Reconfigurable filter bank with complete control over subband bandwidths for multistandard wireless communication receivers," *IEEE Trans. Very Large Scale Integr. (VLSI) Syst.*, 2014, IEEE Xplore, Early Access.
[21] L. R. Rabiner and O. Herrmann, "The predictability of certain optimum finite impulse response digital filters," *IEEE Trans. Circuit Theory*, vol. 20, no. 4, pp. 401–408, Jul. 1973.
[22] T. Coleman, M. A. Branch, and A. Grace, Optimization Toolbox User's Guide, Version 2, MathWorks, Natich, 1999.
[23] B. C. J. Moore, "Perceptual consequences of cochlear hearing loss and their implications for the design of hearing aids," *Ear Hear.*, vol. 17, no. 2, pp. 133–160, Apr. 1996.

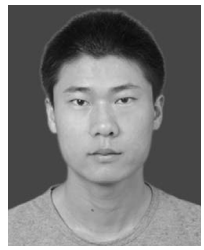

Shaoguang Huang received the B.S. degree from Zhengzhou University, Zhengzhou, China, in 2011.

Currently, he is working toward the M.S. degree at the School of Information Science and Engineering, Shandong University, Jinan, China. His research interests include optimization algorithms, digital filters, and filterbank design.

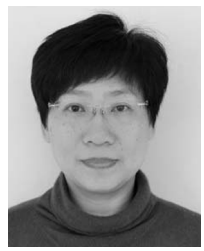

Lan Tian received the B.S. and M.S. degrees from Shandong University, Jinan, China, in 1986 and 1989, respectively, and the Ph.D. degree from Tianjing University, Tianjin, China, in 2009.

Currently, she is a Professor at Shandong University. Her main research interests include acoustic signal processing and cochlea implants.

Xiaojie Ma received the M.B.B.S. and M.D. degrees from Shandong University, Jinan, China, in 1998 and 2003, respectively.

Currently, she is an Attending Physician in the area of otolaryngology at Qilu Hospital of Shandong University. She is mainly engaged in otology clinical work and related basic research.

Ying Wei (M'04) received the B.S. and M.S. degrees from Xi'an Jiaotong University, Xi'an, Shaanxi, China, in 2000 and 2003, respectively, and the Ph.D. degree from the National University of Singapore, Singapore, in 2008.

She worked as a Research Fellow in the Department of Electrical Engineering, National University of Singapore, from 2008 to 2009. In 2010, she joined Shandong University, Jinan, China, as an Associate Professor in the School of Information Science and Engineering. Her research interests include digital filter design, implementation of high-speed digital systems, and biomedical signal processing. She has served in technical program committees, organizing committees, and session chairs for some international conferences.